



Research article

Inhaled exposure to air fresheners aggravated liver injury in a murine model of nonalcoholic fatty acid liver disease

Sanghwa Kim, Ah Young Lee, Myung-Haing Cho^{*}

Laboratory of Toxicology, College of Veterinary Medicine, Seoul National University, Seoul, Republic of Korea

ARTICLE INFO

Keywords:

Air fresheners
Indoor air pollution
High-fructose diet
NAFLD
NASH

ABSTRACT

At present, the consumption and use of air fresheners (AFs) is rapidly increasing worldwide for the purposes of odor removal and to create a pleasant odor. Many recent studies have strongly suggested that the potentially hazardous chemicals emitted from AFs may be the primary source of indoor air pollutants and may cause adverse health effects. Despite the presence of hazardous chemicals in AFs, potential adverse health effects and risk assessment of AFs have not yet been established. The incidence of nonalcoholic fatty acid liver disease (NAFLD) around the world is rapidly increasing, as with obesity and diabetes, and is one of the most common causes of liver disease worldwide. Based on the demonstrated evidence that NAFLD could eventually develop into further health complications such as liver failure, cardiovascular disease, liver cirrhosis, or liver cancer, the current study was performed to clarify the relationship between inhaled AF exposure and NAFLD using a high-fructose diet (HFr)-induced murine model. The results from current study clearly demonstrated that AF exposure further exacerbated liver injury in NAFLD-induced mice. Interestingly, the increased expression of fibrosis-related factors and collagen accumulation in the liver of AF-exposed NAFLD-induced mice resulted in nonalcoholic steatohepatitis (NASH)-like phenotype and fibrosis. Taken together, these results strongly suggest that AF exposure may not only induce liver injury but may also exacerbate NAFLD to lead to NASH-like symptoms. Further study is needed to shed light on the detailed mechanisms behind AF-induced liver effects and its potential role in exacerbating NAFLD to more detrimental disease in order to better scientific evidence for risk assessments of indoor AF exposure.

1. Introduction

Several consumer products (candles, air fresheners, liquid diffusers, etc.) are popularly used to remove malodors, improve sanitary conditions, or to add sensory appeal to indoor spaces. Out of many of these commercial products, around 70% of the U.S. populations have shown to use air care products such as air fresheners (AFs) in 2019 [1,2]. In Korea, the importance placed on indoor air care is increasing and, the AF market has increased roughly three-fold compared to 10 years ago, with an annual growth rate of 8.8% [3, 4]. Although there is an increase in the use of these products and corresponding increased exposure to chemicals, users generally believe that their average exposure level may not be harmful [5]. However, number of studies has identified multiple potential hazardous compounds, such as volatile organic compounds (VOCs) in AFs that may lead to harmful health effects [3, 6]. Volatile organic compounds, including and not limited to benzene, ethylene, toluene, and limonene, are known to be responsible for a range of health conditions,

including nausea, headaches, sensory irritation, and even damage to the organs such as the central nervous system, kidneys, and liver [3]. Presently, very little is known about potential adverse health effects due to exposure to indoor AF products.

Nonalcoholic fatty acid liver disease (NAFLD) is one of the most common liver diseases, in general, the incidence of NAFLD is increasing in Western-style life due to over-eating and a sedentary lifestyle, and an increasing pattern of NAFLD-related diseases is also being observed in Korea [7].

Recent studies have reported that excessive fructose intake is considered a major risk factor for NAFLD and various metabolic disorders [8, 9]. Nonalcoholic fatty acid liver disease consists of a spectrum of phenotypes ranging from simple steatosis to nonalcoholic steatohepatitis (NASH) and liver cirrhosis. Fortunately, NAFLD is known to be reversible, and is usually less dangerous than NASH and liver cirrhosis [10]. However, approximately 15% of NAFLD patients gradually worsen to NASH diagnosis [11]. In general, this progression to NASH can be

^{*} Corresponding author.

E-mail address: mchotox@snu.ac.kr (M.-H. Cho).

<https://doi.org/10.1016/j.heliyon.2021.e06452>

Received 14 October 2020; Received in revised form 12 February 2021; Accepted 4 March 2021

2405-8440/© 2021 The Author(s). Published by Elsevier Ltd. This is an open access article under the CC BY-NC-ND license (<http://creativecommons.org/licenses/by-nc-nd/4.0/>).

explained by the 'two-hit hypothesis' model, which is divided into the 'first-hit' and 'second-hit' stages. The 'first-hit' generally represents hepatic steatosis, while the 'second-hit' explains inflammation, oxidative stress, or liver fibrosis, ultimately leading to complex diseases including NASH [12, 13]. Therefore, hepatic inflammation and liver fibrosis are major features of NASH [13]. When NAFLD progresses to NASH, further complications such as fibrosis, liver failure, liver cirrhosis, and liver cancer are likely to occur [14].

The increasing incidence of NAFLD and the fast-growing AF market in Korea and the world necessitated the present study to elucidate the effects of inhaled AFs on a high-fructose diet (HFr)-induced murine model of NAFLD. The results clearly demonstrated that AF exposure induced severe hepatic damage and liver fibrosis in HFr-fed mice, which are known to be NASH-like phenotypes characterized by hepatic steatosis, inflammation, and liver fibrosis.

2. Materials and Methods

2.1. Materials and analysis of VOCs in AF

The AF product chosen was one of the most commonly-used such products in Korea and was purchased from a local market. To analyze the VOCs emitted from the AF, the air from the purchased AF was collected twice a week during the inhalation experiment. The air samples were collected using a vacuum sampler bag (AVS-550 model, ACEN Co., Korea) connected to gas sampling bags (Tedlar bag, LK Lab Korea, Korea). The vacuum sampler bag was connected to the exhaust port of the chamber and operated at ~3 mL/min. Volatile organic compounds emitted from the AF were analyzed using a Thermal Desorption Gas Chromatograph Mass Spectrometer [(TDS-GC/MS, Agilent Technologies, CA, USA)] by the National Instrumentation Center for Environmental Management (NICEM) of Seoul National University, Seoul, Korea (nicem.snu.ac.kr).

2.2. Animal experiments and treatments

Experiments were conducted on 4-week-old male C57B/L6 mice purchased from Jungang Lab Animal Inc. (Korea). Animals were maintained under constant environmental conditions, with a standard temperature of $20 \text{ }^{\circ}\text{C} \pm 2 \text{ }^{\circ}\text{C}$ and a relative humidity of $50\% \pm 10\%$, under a 12 light/dark cycle. Body weight and the amount of diet consumed were measured twice a week. Based on the methodology outlined in [15], the HFr-induced NAFLD model was established using an HFr diet for 8 weeks before the inhalation experiment. The HFr diet contained 19% protein, 67% carbohydrates, 4% fat, and 700 g fructose per 1,000 g. All mice were randomly divided into the following four treatment groups of five mice each: control (normal diet; D12450K, Research Diets, NJ, USA); AF⁺ (inhaled AF and normal diet); HFr⁺ (HFr diet); and AF⁺/HFr⁺ (inhaled AF and HFr diet); total 20 mice. Each group of mice was fed a normal diet or an HFr diet for a total of 12 weeks. The AF was delivered to the animals in nose-only chambers using a model 108 Atomizer (GreenSolus, Korea). The inhalation experiment was conducted according to the Organization for Economic Co-operation and Development (OECD) guidelines TG 412 (OECD, 2009). In detail, the experiment was designed to fully characterize test material toxicity by repeated inhalation exposure for 28 days. The mice are exposed to 4 hr per day, 5 days per week for 28 days. All experiments were approved by the Internal Animal Care and Use Committee (IACUC) of Seoul National University (SNU-161021-1).

2.3. Western blot assay

The liver tissue of each mouse was homogenized, and total protein concentration was determined using Pierce BCA protein assay kits (Thermo Fisher, Rockford, IL, USA). The membranes were blocked and incubated with primary antibodies. Primary antibodies against phospho-IκB, p-p65, COX-2, SOD1, SOD2, TIMP-1, and β-actin were acquired from

Santa Cruz Biotechnology (Santa Cruz, CA, USA), and primary antibodies against phospho-AMPK, AMPK, LPL, and α-SMA were obtained from Cell Signaling Technology (Danvers, MA, USA). In addition, secondary antibodies were purchased from AbFrontier (Seoul, Korea). Western blotting was performed using an Ez-Capture MG image analyzer (ATTO, Tokyo, Japan), and the western blot bands were analyzed using 3.0 CS analyzer software (ATTO).

2.4. Quantitative RT-PCR

RNA was isolated from frozen liver tissues using the Quick Gene RNA kit (Fujifilm Life Science, Tokyo, Japan), according to the manufacturer's protocol. cDNA was produced using the SuPrimeScript RT Premix (GeNet Bio, Seoul, Korea) and qRT-PCR was performed using the CFX96T Real-time System (Bio-Rad, Hercules, CA, USA). PCR was performed according to the manufacturer's protocol. Actin was used for the relative quantification of the target mRNA.

2.5. Histopathological assays

Liver tissues were fixed in 10% formalin and embedded in paraffin for histological evaluation. The paraffin liver samples were cut into 4 μm-thick sections and prepared on glass slides (Thermo Fisher Scientific, Waltham, MA, USA). The sections were stained with hematoxylin and eosin (H&E) for histopathological examinations and with Picro sirius red (Sigma-Aldrich, St. Louis, MO, USA) to evaluate collagen accumulation. The process was performed according to the methodology described previously [15]. The slides were then incubated with F4/80 antibodies (Abcam, Cambridge, UK) and 3% bovine serum albumin (BSA) overnight at 4 °C. After these steps, the slides were incubated with HRP-conjugated secondary antibodies. The sections were washed and incubated with 3, 3'-diaminobenzidine hydrochloride (DAB) substrate kits (Invitrogen, Carlsbad, CA, USA) for immunohistochemistry (IHC) analysis. The slides were imaged under a light microscope (Nikon, Tokyo, Japan). Macrosteatosis was analyzed as macrovesicular and was objectively quantified as surface area of macrovesicular using ImageJ software (NIH; imagej.nih.gov/ij/index.html). The measurements were normalized to the average of liver sections from the control group.

2.6. Biochemical analyses

Blood samples were centrifuged at 12,000 rpm for 60 min and the supernatant was collected as the serum. The serum AST, ALT, TC, and TG levels were analyzed by the Neodin Medical Institute (Seoul, Korea). Whole blood samples were used to analyze hemoglobin A1c (HbA1c) and insulin levels using commercial ELISA kits (Koma Biotech, Seoul, Korea). Fasting glucose concentration was measured using an Accu-Chek glucometer (Roche, Basel, Switzerland) after fasting for 6 hr.

Insulin resistance (IR) was calculated using the following formula: HOMA (Homeostatic Model Assessment)-IR = [fasting glucose (nmol/L) × insulin (μU/mL)/22.5]. Insulin sensitivity (IS) was calculated using the following formula: IS = 1/IR.

2.7. ELISA assays

Mouse TNF-α and IL-6 Quantikine ELISA kits were purchased from R&D Systems (Minneapolis, MN, USA). Mouse serum samples were collected from blood samples by centrifugation at 12,000 rpm for 60 min. The ELISA assay was conducted according to the manufacturer's instructions. The intrahepatic triglyceride and fructose contents were determined using EnzyChrom™ assay kits (BioAssay Systems, Hayward, CA, USA). Mouse insulin ELISA kits (Koma Biotech, Seoul, Korea) were used to analyze insulin levels in the intrahepatic samples.

2.8. Statistics analysis

Data were analyzed using an independent samples *t*-tests (GraphPad Software, CA, USA) and results are reported as means \pm SD. Significance levels were set at $P^* < 0.05$, $P^{**} < 0.01$, and $P^{***} < 0.001$. The experiments were performed at least 3–5 analysis in each set of experiments.

3. Results

3.1. Identification of AF ingredients under experimental conditions

As described in the Materials and Methods section, VOCs were measured from the AF inhalation chamber during experiments. All VOCs identified in the AF exposure chamber during the experiment can be found in the Excel file within the supplementary data. Based on the findings of [3], the major VOCs frequently detected in AF exposure inhalation chambers are summarized in Table 1. The total amount of VOCs (TVOCs) was measured to be $4,808 \pm 801 \mu\text{g}/\text{m}^3$, (mean \pm SD of 8 independent experiments). In particular, the most frequently detected components from the AF were linalool and phenol during the experiment. Additionally, various terpenes, including *d*-limonene and α -pinene, and 5 other VOCs, such as xylene and styrene, were also detected.

3.2. AF exposure promotes hepatic steatosis in both normal diet- and HFr-fed mice

The NAFLD model mice and normal diet mice were exposed to AF for 4 hr/day, 5 days/week, for a total of 28 days, according to the OECD guidelines, as described in the Methods section (Figure 1A). Body weight change showed that the mean body weights of the HFr⁺, AF⁺, and AF⁺/HFr⁺ groups were lower than those of the control group during the experimental period. In particular, the body weight of the AF⁺/HFr⁺ group was dramatically decreased after 8 weeks compared to that of the other groups (Figure 1B). As shown in Table 2, although no statistically significant differences were detected for cumulative food intake, the total body weight gain was reduced significantly in the AF⁺/HFr⁺ group compared to the control group (Table 2). In addition, the expression of Glut 2, which participates in fructose transport into hepatocytes, was increased in the AF⁺/HFr⁺ group (Figure 1C). This also corresponded with increased-fructose level in the liver of the high fructose-fed mice groups (Figure 1D). The liver sections of the HFr⁺ and AF⁺/HFr⁺ groups demonstrated hepatic steatosis-like phenotypes such as hepatocellular ballooning, compared to the control group and hepatocytes with ballooning under H&E staining were particularly common in the HFr⁺/AF⁺ exposure group (Figure 1E, thick arrows in HFr⁺, HFr⁺/AF⁺ group). Interestingly, the hepatocytes of the AF⁺ group were packed loosely (Figure 1E, thin arrows in the AF⁺ group). Hepatocytes with ballooning were analyzed in the liver sections and were quantified using ImageJ (Figure 1F) [16]. Investigating the induction of gluconeogenesis, G6pase, and fatty acid synthase (FAS) mRNA expression levels, demonstrated that the numbers of representative gluconeogenesis markers were clearly

elevated in the HFr⁺/AF⁺ group compared to the control group (Figure 1G).

To evaluate accumulation of lipids in the livers, the total cholesterol (TC) (Figure 1I) and triglyceride (TG) (Figure 1J) contents were analyzed in bloods. As the results, TC and TG levels were significantly increased in the exposure to HFr⁺/AF⁺ mice groups. The intrahepatic triglyceride contents were also increased by exposure to AF, especially pronounced in the HFr⁺/AF⁺ group (Figure 1K).

3.3. Exposure to AF induces insulin resistance in normal diet-fed mice as well as in HFr-fed mice

Inhalation exposure to AF induced high insulin concentrations in both the normal diet- and the HFr-fed mice (Figure 2A), suggesting that insulin resistance was induced. Reduced insulin resistance was further confirmed by the observed increase in homeostatic model assessment for insulin resistance (HOMA-IR, Figure 2B) and decrease in insulin sensitivity (Figure 2C). As HOMA-IR is generally associated with diabetes and metabolic syndromes, its diagnosis seems pertinent during the evaluation of insulin sensitivity [15]. Figure 2D shows the measured HbA1c levels, which are a diagnostic index of diabetes, and a slight increase in the HbA1c level was observed in the AF⁺/HFr⁺ group compared to the other experimental treatments (Figure 2D).

3.4. Exposure to AF induces generation of reactive oxygen species (ROS) and hepatic inflammation in HFr-fed mice

To evaluate the extent of ROS generation and AF-induced oxidative stress, the expression levels of oxidative stress-related proteins such as superoxide dismutase 1 (SOD1), SOD2, and cyclooxygenase-2 (COX-2) were measured. The results indicated that all the expression levels were increased by AF exposure. Exposure to AF clearly increased oxidative stress, especially in HFr-fed mice (Figure 3A). The fact that changes in oxidation-reduction homeostasis can lead to endoplasmic reticulum (ER) stress under high fructose uptake [15]. The data clearly demonstrated that AF exposure increased the levels of ER stress-related proteins, particularly in HFr-fed mice (Figure 3B). To evaluate inflammatory responses to AF exposure, the levels of pro-inflammatory cytokine markers such as tumor necrosis factor- α (TNF- α), and interleukin-6 (IL-6), and interleukin-10 (IL-10) were analyzed. The results showed that TNF- α levels were slightly increased in HFr-fed mice, however, AF co-exposure did not significantly affect the level of TNF- α (Figure 3C). Air freshener-induced effects on TNF- α mRNA level are shown in Figure 3D. Air freshener inhalation increased the TNF- α mRNA level, and AF-induced effects were clearly observed in the HFr-fed group, suggesting post-transcriptional modification of TNF- α expression. This phenomenon should be further investigated, as this was beyond the scope of the current study. The effects of AF inhalation on IL-6 levels in HFr-fed mice were also demonstrated. As shown in Figure 3E and F, AF exposure increased IL-6 levels, especially in HFr-fed mice, and additional mRNA analysis demonstrated that AF exposure itself and co-exposure with HFr distinctly increased IL-6 levels. Further study is needed to

Table 1. List of representative volatile organic compounds (VOCs) emitted from the tested air freshener under experimental conditions.^{a,b}

	Phenol ($\mu\text{g}/\text{m}^3$)	Terpenes ($\mu\text{g}/\text{m}^3$)			Toluene ($\mu\text{g}/\text{m}^3$)	Xylene ($\mu\text{g}/\text{m}^3$)	TVOCs ($\mu\text{g}/\text{m}^3$) ^c
		Linalool	<i>d</i> -limonene	α -pinene			
Air freshener	947.27 \pm 173.78	480.87 \pm 213.52 ^d	325.39 \pm 510.33 ^d	15.2 \pm 5.2 ^d	33.3 \pm 14.48 ^d	1.7 \pm 4.86 ^d	4,808.9 \pm 801.54 ^d

^a The samples were collected in vacuum sampler bags with Tedler bags (10L) connected to the exhaust port of the inhalation chamber. The vacuum sampler bag operated at ~ 3 mL/min. Volatile organic compounds emitted from the AF were analyzed using TDS-GC-MSD in NICEM of Seoul National University. Samples were collected eight times during individual experiments.

^b Table 1 represents VOCs that were frequently detected in AFs or were detected at high concentrations. In addition, 5VOCs such as toluene and xylene were detected in the AF.

^c TVOCs: Total VOCs, the list of all VOCs detected in the AF, is attached to the Excel file entitled 'identification of AF ingredients.'

^d Mean \pm SD (n = 8).

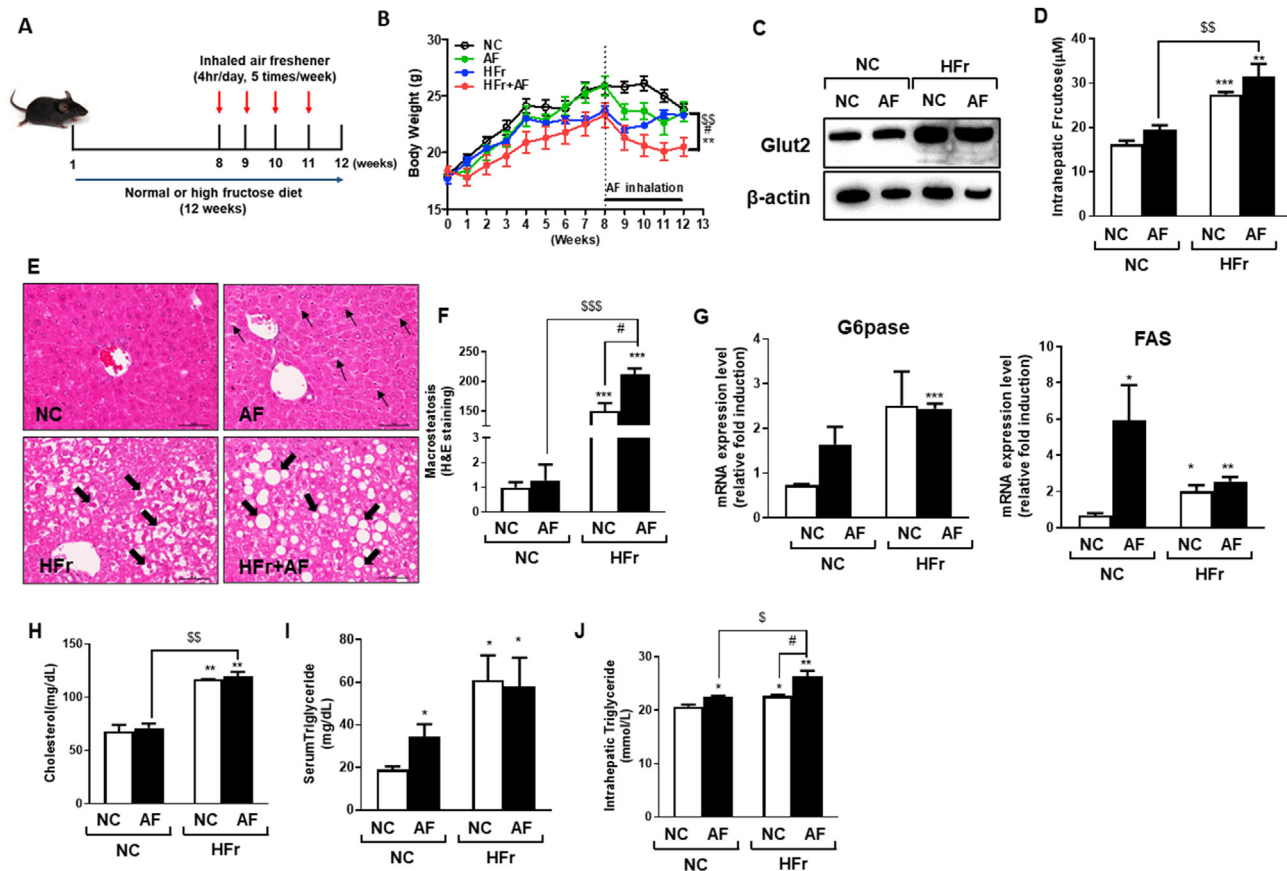


Figure 1. Air freshener exposure promotes hepatic steatosis in HFr-fed mice (A) Diagram of the animal experiment during the study. (B) The change in body weight during the experimental period. (C) The expression of Glut 2. (D) ELISA analysis of intrahepatic fructose. (E) H&E staining of the liver. Thick arrows indicate ballooning degeneration, characterized by cytoplasm swelling, whereas thin arrows indicate loosely packed hepatocytes (magnification 20X). (F) Summary of the hepatocyte ballooning index taken from H&E staining. (G) mRNA expression levels of the G6pase and FAS gluconeogenesis markers. (H) The levels of total cholesterol (TC) in the blood. (I) The levels of serum triglyceride (TG) in the blood. (J) ELISA analysis of intrahepatic triglyceride (TG). Data are expressed as means \pm SD ($n = 3\sim 5$); * $P < 0.05$, ** $P < 0.01$, and *** $P < 0.001$ compared to the control (AF⁻/HFr⁻) group. ^S $P < 0.05$, ^{SS} $P < 0.01$ and ^{SSS} $P < 0.001$ compared to the AF group. # $P < 0.05$ compared to the HFr group.

determine the underlying mechanisms behind this finding. In contrast, the levels of IL-10, an anti-inflammatory marker, were decreased in both the AF⁺ and AF⁺/HFr⁺ groups (Figure 3G). IL-10 downregulates the expression of Th1 cytokines, MHC class II antigens, and co-stimulatory molecules on macrophages. As the results, IL-10 can block NF- κ B activity and is involved in the regulation of the JAK-STAT signaling pathway [17]. TNF- α is a major pro-inflammatory cytokine that activates the NF- κ B pathway and regulates inflammation responses [18, 19]. Inhaled AF exposure under the HFr diet clearly increased the expressions of NF- κ B pathway-related proteins, such as phospho-I κ B α and phospho-p65 (Figure 3H), which are involved in the NF- κ B

pathway-related inflammation response [19]. Finally, a greater number of F4/80-positive macrophages were detected in the AF⁺, HFr⁺, and AF⁺/HFr⁺ groups compared to the control (Figure 3I; thin arrows).

3.5. Exposure to AF leads to liver fibrosis in HFr-fed mice, which presents a NASH-like phenotype

Excessive nutrient intake stimulates hepatic steatosis which may severely progress into NASH, liver cirrhosis, and chronic liver diseases [7, 20]. To investigate potential liver injuries caused by AF exposure in NAFLD mice, AST and ALT levels were measured. The results indicated

Table 2. The effects of air freshener inhalation on the metabolic profiles of normal and HFr-fed mice.^a

	AF/HFr ⁻	AF ⁺	HFr ⁺	AF ⁺ /HFr ⁺
Body weight (0W, g)	18.8 \pm 1.1	17.8 \pm 1.3	17.4 \pm 1.7	18.1 \pm 0.7
Body weight (12W, g)	23.8 \pm 1.3	23.5 \pm 2.2	23.3 \pm 0.8	20.5 \pm 2.5***##SSS
Cumulative food intake (g/12w)	251.9 \pm 78.3	267.47 \pm 84.6	204.91 \pm 81.1	181.72 \pm 88.7
Total Energy intake (Kcal/12w)	968 \pm 301	1027 \pm 325.2	787.5 \pm 311.4	698.4 \pm 341

*** $p < 0.001$ compared to the control group (AF⁻/HFr⁻), ## $p < 0.001$ compared to the AF⁺ group, SSS $p < 0.001$ compared to the HFr⁺ group.

^a Mean \pm SD ($n = 3\sim 5$).

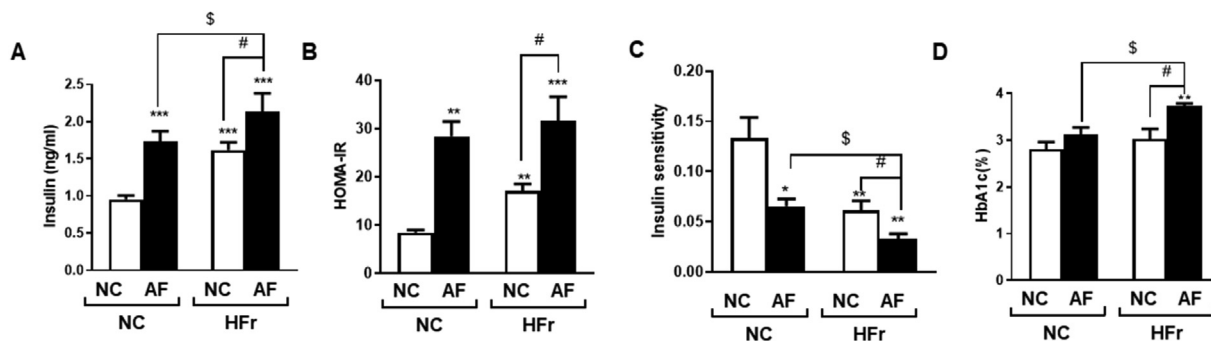


Figure 2. Air freshener exposure induces insulin resistance in normal diet-fed mice as well as in HFr-fed mice (A) The levels of insulin in the blood. (B) Measurement of HOMA-IR. (C) Measurements of insulin sensitivity. (D) HbA1c levels in the blood. Data are expressed as means \pm SD ($n = 3-5$); * $P < 0.05$, ** $P < 0.01$, and *** $P < 0.001$ compared to the control group. $^{\$}P < 0.05$ compared to the AF group. $^{\#}P < 0.05$ compared to the HFr group.

that the levels were elevated in the AF⁺/HFr⁺ group (Figure 4A and B) and histopathologically, collagen accumulation was indicated in the AF⁺/HFr⁺ group by a red signal from the sirius red staining (Figure 4C; thin arrows). In addition, the expressions of fibrosis markers such as α -SMA and TIMP-1 were upregulated in the AF⁺ group, and this intensity was clearly observed in the AF⁺/HFr⁺ group (Figure 4D).

4. Discussion

The continuing trend for personal use of AFs at the global level has been increasing markedly year-on-year. Air fresheners are not only used for air care (malodor management), deodorant, and fragrance, but also for interior decoration (candles, votive and diffusers). The use of AFs has dramatically increased not only in homes, but also in offices, public places, and cars in Korea as well [21]. Evidence from previous studies has shown that AFs contain various toxic chemicals including benzene, limonene, xylene, aldehyde, and toluene [4, 6]. These chemicals can represent health hazards such as dermal allergic responses, and can lead to local sensory irritation, and even systemic toxicity [4]. However,

despite the increasing use of AFs worldwide and increasing concerns over the potential for systemic toxicity of AF-containing ingredients, most compounds contained in AFs are not labeled as human health hazards on the product label. In addition, there are a lack of risk assessments and user guidelines for using AFs. The general population may be exposed to a large amount of chemical mixtures, thus raising valid concerns over potential impacts on human health with continued exposures [22]. The analysis of the AF exposure inhalation chamber carried out in the present study revealed that multiple chemical mixtures were present (Table 1 and supplementary data of excel). In general, VOCs may be divided into those that are harmful or beneficial to humans, and the total VOCs (TVOCs) index in the current study encompasses both types. The analysis in the present study detected harmful VOCs, such as xylene and styrene, as well as beneficial VOCs, such as terpene-based VOCs, in air fresheners (Table 1 and supplementary data of excel). At present, there are no reliable risk assessment techniques concerning this exposure to multiple chemicals or co-exposure to multiple chemicals that are covered by a regulatory framework. For this reason, it is necessary to develop methodologies to better assess the potential toxicity of chemical mixtures in the form of

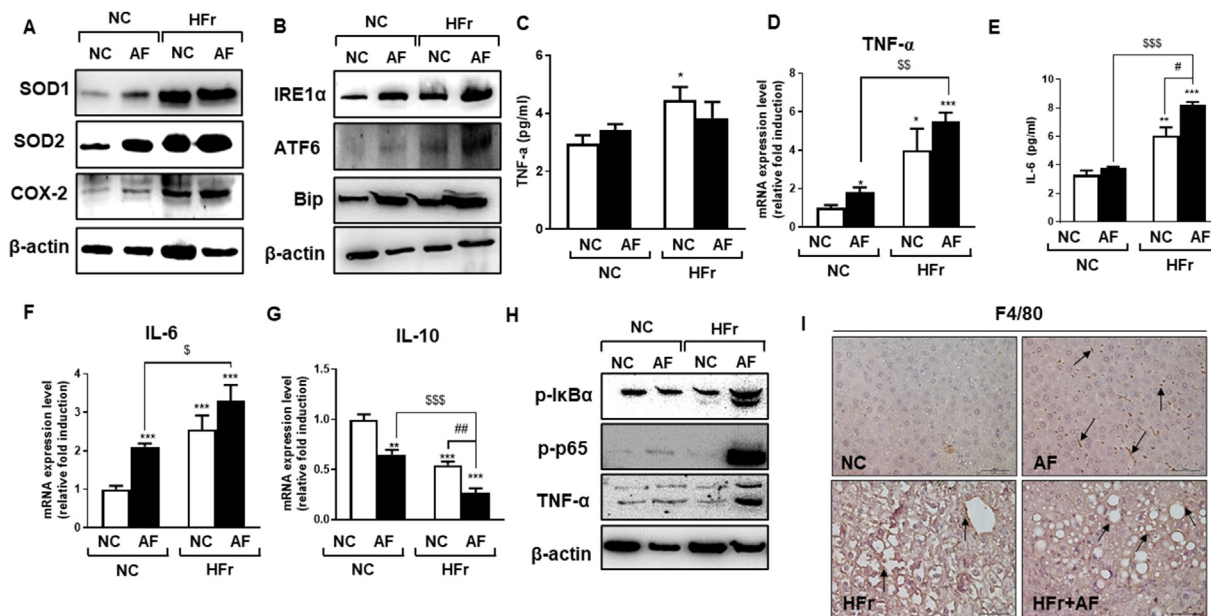


Figure 3. Air freshener exposure induces ROS and hepatic inflammation in HFr-fed mice. The expression levels of (A) oxidative stress-related proteins; SOD1, SOD2, and COX-2 and (B) ER stress-related proteins; IRE1 α , ATF6, and GRP78/Bip. (C) ELISA analysis of TNF- α in the serum. (D) TNF- α mRNA level. (E) ELISA analysis of IL-6 in the serum. mRNA levels of (F) IL-6 and (G) IL-10. (H) The expression levels of inflammation-related proteins; p-IkB, p-p65, and TNF- α . (I) The expression of the F4/80 macrophage marker in the liver by IHC (F4/80 indicated by thin arrows, magnification 20x). Data are expressed as means \pm SD ($n = 3-5$); * $P < 0.05$, ** $P < 0.01$, and *** $P < 0.001$ compared to the control group. $^{\$}P < 0.05$, $^{\$\$}P < 0.01$ and $^{\$\$\$}P < 0.001$ compared to the AF group. $^{\#}P < 0.05$ and $^{\#\#}P < 0.01$ compared to HFr group.

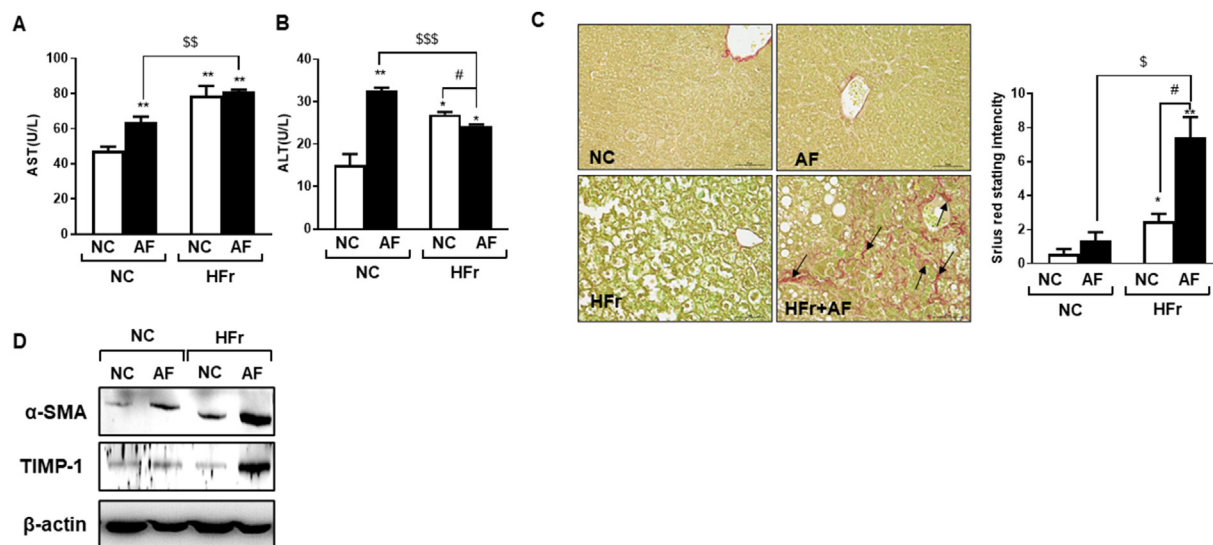


Figure 4. Exposure to AF leads to liver fibrosis in HFr-fed mice. The levels of (A) AST and (B) ALT in the blood. (C) Representative collagen accumulation in livers of experimental mice determined by sirius red staining (collagen accumulation indicated by thin arrows, left panel) and the intensity of the red signal (right panel, magnification 20x). (D) The expression levels of the α -SMA and TIMP-1 fibrosis markers. Data are expressed as means \pm SD ($n = 3\text{--}5$); * $P < 0.05$ and ** $P < 0.01$ compared to the control (AF⁻/HFr⁻) group. $^{\$}P < 0.05$, $^{\$\$}P < 0.01$ and $^{\$ \$ \$}P < 0.001$ compared to the AF group. $^{\#}P < 0.05$ compared to the HFr group.

newly integrated models for exposure assessment. These new assessments should focus not only on *in silico*, *in vitro* and *in vivo* effects, but also on integrated epidemiological-toxicological approaches for assessing the risk of chemical mixtures and on prioritizing mixtures of concern [22]. As shown in Figure 1E, compared to the control groups, hepatocytes were loosely packed in AF-exposed mice fed a normal diet, suggesting that AF exposure exacerbates steatosis-like phenotypes. Typical features of a simple steatosis-like phenotype can be characterized by hepatocellular ballooning and fat accumulation because the hepatocytes become loose due to the fat accumulated between the portal veins [8, 23]. As shown in Figure 1, the results of the present study also demonstrated that AF exposure caused simple steatosis-like phenotypes and that co-exposure with HFr aggravated the phenotype in the murine model.

Although NAFLD is classified as a reversible condition, it is known to be a risk factor for fibrosis, hypertension, and cardiovascular diseases because NAFLD can worsen to more serious conditions such as NASH, liver cirrhosis, and even hepatocellular carcinoma [11, 24]. Therefore, it is quite desirable to evaluate various metabolic risk factors for better and accurate diagnosis.

In the Asia-Pacific region, around 25% of NAFLD cases progress from simple steatosis to NASH and develop into advanced liver fibrosis in 3 years [20]. Nonalcoholic steatohepatitis is histologically characterized by a steatosis phenotype, inflammation, hepatic injury, and the progression of fibrosis [10, 13]. As mentioned earlier, our scientific purpose of this study was to evaluate potential effects of fast-growing AF products on the increasing incidence of NAFLD. This is why we established the HFr-induced metabolic disorder mice to be applicable to AF inhalation.

In the current study, exposure to a mixture of AF was accompanied by generation of ROS, inflammatory responses, and even liver fibrosis, causing more severe liver damage (Figures 3 and 4). Intriguingly, when normal diet-fed mice were exposed to AF, only steatosis was impaired without the progression of an inflammatory response and hepatocyte fibrosis. However, AF exposure under the HFr-diet led to the development of histopathological features of NASH with the progression of inflammation and extensive fibrosis. Additionally, the progression of NASH with fibrosis was observed in a murine model under AF exposure. This is the first study demonstrating that inhaled AF may lead to the development of an aggressive NASH phenotype in a murine model of NAFLD. These results strongly suggest that AF exposure may cause

adverse health effects under the tested experimental conditions. However, further studies are needed to elucidate the detailed mechanisms behind these potential adverse effects on human health. Recently, many researchers investigate the health impact of toxic compounds contained in AFs under indoor environments. The approach discussed in this study may be used to establish improved guidelines for the safety assessment of diverse indoor consumer products.

In summary, the current study demonstrated that a mixture of diverse chemicals emitted from an AF caused and aggravated liver damage in a NAFLD murine model. Further study is clearly needed to provide scientific data for reliable risk assessments and to develop user guidelines for multiple chemical mixtures such as those found in AFs.

Declarations

Author contribution statement

Sanghwa Kim: Conceived and designed the experiments; Performed the experiments; Analyzed and interpreted the data; Contributed reagents, materials, analysis tools or data; Wrote the paper.

Ah Young Lee: Performed the experiments; Contributed reagents, materials, analysis tools or data.

Myung-Haing Cho: Conceived and designed the experiments; Wrote the paper.

Funding statement

SH Kim and AY Lee were partially supported by BK21 PLUS Program for Creative Veterinary Science Research.

Data availability statement

Data included in article/supplementary material/referenced in article.

Declaration of interests statement

The authors declare no conflict of interest.

Additional information

Supplementary content related to this article has been published online at <https://doi.org/10.1016/j.heliyon.2021.e06452>.

Acknowledgements

We would like to express special thanks to Dr. Christopher Choi for his careful manuscript review.

References

- [1] M.B. Johnson, R. Kingston, M.J. Utell, J.R. Wells, M. Singal, W.R. Troy, S. Horezniak, P. Dalton, F.K. Ahmed, R.S. Herz, T.G. Osimitz, S. Praver, S. Yin, Exploring the science, safety, and benefits of air care products: perspectives from the inaugural air care summit, *Inhal. Toxicol.* 31 (2019) 12–24.
- [2] B.C. Singer, H. Destailats, A.T. Hodgson, W.W. Nazaroff, Cleaning products and air fresheners: emissions and resulting concentrations of glycol ethers and terpenoids, *Indoor Air* 16 (2006) 179–191.
- [3] S. Kim, S.H. Hong, C.K. Bong, M.H. Cho, Characterization of air freshener emission: the potential health effects, *J. Toxicol. Sci.* 40 (2015) 535–550.
- [4] W.K. Jo, J.H. Lee, M.K. Kim, Head-space, small-chamber and in-vehicle tests for volatile organic compounds (VOCs) emitted from air fresheners for the Korean market, *Chemosphere* 70 (2008) 1827–1834.
- [5] F. Ibrahim Alshaer, D. Fuad Albaharna, H.O. Ahmed, M. Ghiyath Anas, J. Mohammed Aljassmi, Qualitative analysis of air freshener spray, *J. Environ. Publ. Health* 2019 (2019) 9316707.
- [6] P. Wolkoff, G.D. Nielsen, Effects by inhalation of abundant fragrances in indoor air – an overview, *Environ. Int.* 101 (2017) 96–107.
- [7] J.J. Yoo, W. Kim, M.Y. Kim, D.W. Jun, S.G. Kim, J.E. Yeon, J.W. Lee, Y.K. Cho, S.H. Park, J.H. Sohn, Recent research trends and updates on nonalcoholic fatty liver disease, *Clin. Mol. Hepatol.* 25 (2019) 1–11.
- [8] J.P. Bantle, Dietary fructose and metabolic syndrome and diabetes, *J. Nutr.* 139 (2009) 1263s–1268s.
- [9] T. Jensen, M.F. Abdelmalek, S. Sullivan, K.J. Nadeau, M. Green, C. Roncal, T. Nakagawa, M. Kuwabara, Y. Sato, D.H. Kang, D.R. Tolan, L.G. Sanchez-Lozada, H.R. Rosen, M.A. Lanaspa, A.M. Diehl, R.J. Johnson, Fructose, sugar, A major mediator of non-alcoholic fatty liver disease, *J. Hepatol.* 68 (2018) 1063–1075.
- [10] Nonalcoholic Fatty Liver Disease & NASH, National Institute of Diabetes and Digestive and Kidney Diseases, 2020.
- [11] R.S. Sharma, D.J. Harrison, D. Kisielowski, D.M. Cassidy, A.D. McNeilly, J.R. Gallagher, S.V. Walsh, T. Honda, R.J. McCrimmon, A.T. Dinkova-Kostova, M.L.J. Ashford, J.F. Dillon, J.D. Hayes, Experimental nonalcoholic steatohepatitis and liver fibrosis are ameliorated by pharmacologic activation of Nrf 2 (NF-E2 p45-related factor 2), *Cell. Mol. Gastroenterol. Hepatol.* 5 (2018) 367–398.
- [12] Y. Qiu, Z. Zheng, H. Kim, Z. Yang, G. Zhang, X. Shi, F. Sun, C. Peng, Y. Ding, A. Wang, L.C. Chen, S. Rajagopalan, Q. Sun, K. Zhang, Inhalation exposure to PM2.5 counteracts hepatic steatosis in mice fed high-fat diet by stimulating hepatic autophagy, *Sci. Rep.* 7 (2017) 16286.
- [13] Z. Zheng, X. Xu, X. Zhang, A. Wang, C. Zhang, M. Hüttemann, L.I. Grossman, L.C. Chen, S. Rajagopalan, Q. Sun, K. Zhang, Exposure to ambient particulate matter induces a NASH-like phenotype and impairs hepatic glucose metabolism in an animal model, *J. Hepatol.* 58 (2013) 148–154.
- [14] M.E. Rinella, A.J. Sanyal, Management of NAFLD: a stage-based approach, *Nat. Rev. Gastroenterol. Hepatol.* 13 (2016) 196–205.
- [15] S. Kim, A.Y. Lee, H.J. Kim, S.H. Hong, R.E. Go, K.C. Choi, K.S. Kang, M.H. Cho, Exposure to cigarette smoke disturbs adipokines secretion causing intercellular damage and insulin resistance in high fructose diet-induced metabolic disorder mice, *Biochem. Biophys. Res. Commun.* 494 (2017) 648–655.
- [16] D. Sethunath, S. Morusu, M. Tuceryan, O.W. Cummings, H. Zhang, X.M. Yin, S. Vanderbeck, N. Chalasani, S. Gawrieh, Automated assessment of steatosis in murine fatty liver, *PLoS One* 13 (2018), e0197242.
- [17] F. Driessler, K. Venstrom, R. Sabat, K. Asadullah, A.J. Schottelius, Molecular mechanisms of interleukin-10-mediated inhibition of NF- κ B activity: a role for p50, *Clin. Exp. Immunol.* 135 (2004) 64–73.
- [18] S.E. Borst, The role of TNF- α in insulin resistance, *Endocrine* 23 (2004) 177–182.
- [19] T. Liu, L. Zhang, D. Joo, S.-C. Sun, NF- κ B signaling in inflammation, *Signal Transduct. Target. Ther.* 2 (2017) 17023.
- [20] J.G. Fan, S.U. Kim, V.W. Wong, New trends on obesity and NAFLD in Asia, *J. Hepatol.* 67 (2017) 862–873.
- [21] S. Lee, South Korea Releases Consumer Chemical Products Standards, Comprehensive Rules Include Phase-In Safety Checks and Labelling Requirements, 2019.
- [22] S.K. Bopp, R. Barouki, W. Brack, S. Dalla Costa, J.C.M. Dorne, P.E. Drakvik, M. Faust, T.K. Karjalainen, S. Kefalopoulos, J. van Klaveren, M. Kolossa-Gehring, A. Kortenkamp, E. Lebrecht, T. Lettieri, S. Nørgaard, J. Rügge, J.V. Tarazona, X. Trier, B. van de Water, J. van Gils, Å. Bergman, Current EU research activities on combined exposure to multiple chemicals, *Environ. Int.* 120 (2018) 544–562.
- [23] M. Oron-Herman, Y. Kamari, E. Grossman, G. Yeager, E. Peleg, Z. Shabtay, A. Shamiss, Y. Sharabi, Metabolic syndrome: comparison of the two commonly used animal models, *Am. J. Hypertens.* 21 (2008) 1018–1022.
- [24] T. Tsuchida, Y.A. Lee, N. Fujiwara, M. Ybanez, B. Allen, S. Martins, M.I. Fiel, N. Goossens, H.I. Chou, Y. Hoshida, S.L. Friedman, A simple diet- and chemical-induced murine NASH model with rapid progression of steatohepatitis, fibrosis and liver cancer, *J. Hepatol.* 69 (2018) 385–395.